AERODYNAMICS OF CHESTNUT TIGER BUTTERFLY IN FORWARD FLIGHT

Naoto Yokoyama*a), Kei Senda*, Makoto Iima** & Norio Hirai***
**Department of Aeronautics and Astronautics, Kyoto University, Kyoto, 606-8501, Japan*
***Department of Mathematical and Life Sciences, Hiroshima University, Higashi-Hiroshima, 739-8521, Japan*
****Graduate School of Life and Environmental Sciences, Osaka Prefecture University, Sakai, 599-8531, Japan*

Summary Forward flights of a flapping butterfly consisting of rigid bodies are numerically simulated. Coherent vortical structures near the butterfly are visualized. The generation mechanism of the aerodynamic forces due to the large-scale vortical structures are clarified. The small-scale vortical structures on the wings directly affect the pitching angle of the butterfly. The control of the pitching angle is essential for stable periodic flights of butterflies.

INTRODUCTION

Flying animals on the Earth have to produce lift to float against the gravitational force and thrust to fly forward against drag. Moreover, the flyers must control their attitudes during the flights by making appropriate torques. The forces and torques acted on the flyers are made as reactions when the flyers change the momenta and the angular momenta of the surrounding air. Characteristic vortical structures are created by flying animals. Doughnut-shaped vortex rings are often shed by fast-traveling flyers' wings while undulating cylindrical vortices trailing behind each wing tip are often seen in the wakes of the slow-traveling flyers [1]. A ladder-like vortical structure in the wake of a flapping butterfly is proposed [2]. The relation between vortical structures induced by the flappings and aerodynamic forces is experimentally and theoretically investigated [3, 4, 5].

In this work, flapping butterflies in forward flight are numerically simulated to clarify the relation between the aerodynamic forces and the flow structures characterized by vortices. Three kinds of the simulations, distinguished by the way to determine the positions and the attitudes of the thoraxes of the butterflies, are carried out: a tethered simulation, where the thorax of the butterfly is fixed, a prescribed simulation, where the thorax trajectory is given by those observed in the corresponding experiment, and a free-flight simulation, where only the joint angles are given. In the tethered simulation, the forces and the wake structures caused by the flapping are compared with the corresponding experiment. In the prescribed simulation, the vortical structures are visualized and the forces due to the vortical structures are identified. In the free-flight simulation, the desired conditions to realize the free flights are discussed.

NUMERICAL METHOD

The governing equation of the flow is the incompressible Navier–Stokes equation. The flow runs into the computational domain with constant velocities, and the periodic boundary conditions in the directions lateral to the mainstream are employed. The interactions between the flow and the butterfly are calculated by the immersed boundary method [6].

A chestnut tiger butterfly (*Parantica sita*) is modeled as four rigid bodies: a spheroidal thorax, a spheroidal abdomen, and a left and a right thin flat wings. The modeled butterfly has one wing unifying a forewing and a hindwing on one side and the shape of the wings are taken from living butterflies. The thorax has six degrees of freedom (DOF): three DOFs of its center of mass and three DOFs of its attitude. The thorax and the abdomen as well as the thorax and the left and the right wings is connected with three DOF joint. The thorax coordinates $\boldsymbol{\theta}_1 \in \mathbb{R}^6$ and the joint angles $\boldsymbol{\theta}_2 \in \mathbb{R}^9$ constitute generalized coordinates of the butterfly $\boldsymbol{\theta} = (\boldsymbol{\theta}_1, \boldsymbol{\theta}_2) \in \mathbb{R}^{15}$. The state of the butterfly is given by $\boldsymbol{\theta}$ and its time derivative $\dot{\boldsymbol{\theta}}$. The kinematics of the butterfly is expressed by the Lagrangian formalism as follows:

$$\boldsymbol{M}\ddot{\boldsymbol{\theta}} + \dot{\boldsymbol{M}}\dot{\boldsymbol{\theta}} - \frac{1}{2}\frac{\partial}{\partial \boldsymbol{\theta}}\left(\dot{\boldsymbol{\theta}}\boldsymbol{M}\dot{\boldsymbol{\theta}}\right) + \frac{\partial V}{\partial \boldsymbol{\theta}} = \boldsymbol{\tau}, \tag{1}$$

where $\boldsymbol{M}$ is the inertial matrix, and V is the potential energy due to the gravity. The generalized forces $\boldsymbol{\tau}$ are composed of the aerodynamic forces $\boldsymbol{\tau}_{\mathrm{air}}$ and the control forces applied to the thorax and the joints $\boldsymbol{\tau}_{\mathrm{cont}}$.

In all the three simulations, the joint angles $\boldsymbol{\theta}_2$ are given by the experimental observations. In the tethered simulation, $\boldsymbol{\theta}_1 = \mathrm{const.}$ since the thorax is fixed. In the prescribed simulation, $\boldsymbol{\theta}_1$ are given by a free-flight experiment. Both in the tethered and the prescribed simulations, the control forces $\boldsymbol{\tau}_{\mathrm{cont}}$ are given by Eq. (1). In the free-flight simulation, Eq. (1) is solved by the inverse kinematics. Since the butterflies in free flights cannot directly control the thorax, $\boldsymbol{\tau}_{\mathrm{cont1}} = \boldsymbol{0}$. Then, the controllable joint torques $\boldsymbol{\tau}_{\mathrm{cont2}}$ and the acceleration of the thorax $\ddot{\boldsymbol{\theta}}_1$ are analytically given according to Eq. (1). The time development of $\boldsymbol{\theta}_1$ and $\dot{\boldsymbol{\theta}}_1$ during the free-flight simulation is made by a numerical integration.

RESULTS

In this paper, only the results of the prescribed simulation is shown. Lift, drag and pitching moment in the prescribed simulation are shown in Fig. 1. The lift is created during the downstroke ($t < 0.056$s) and the thrust is during the upstroke

a) Corresponding author. E-mail: yokoyama@kuaero.kyoto-u.ac.jp

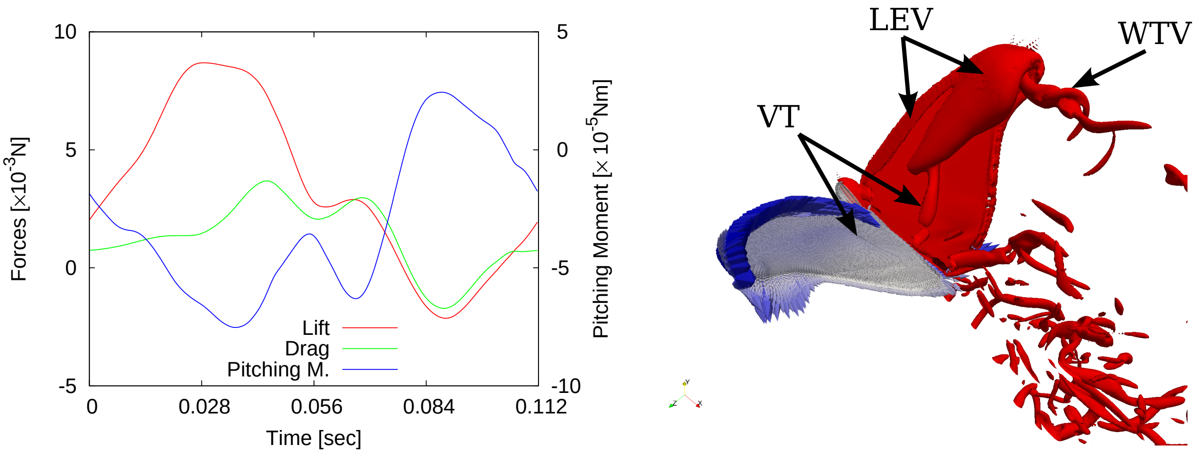

Figure 1. Left: Lift, drag and pitching moment. The pitching moment is scaled by the right-hand axis. Right: Aerodynamic force distribution on the butterfly and vortical structures visualized by the Q-criterion viewed from above and behind.

($t > 0.056$s). The negative pitching moment during the downstroke makes the head down and the positive pitching moment during the upstrokes makes the head up. The extra forces applied to the thorax, which the butterfly can not make, are required to realize the observed trajectory of the butterfly. Although the extra forces are as large as the aerodynamic forces, their powers are much smaller than the powers due to the controllable joints. It suggests that the control to make stable periodic flights is energy-efficient.

The aerodynamic forces acting on the butterfly and characteristic vortical structures visualized with Q-criterion at an early stage of a downstroke are also shown in Fig. 1. Leading-edge separation makes strong leading-edge vortices (LEV). The wingtip vortices (WTV) made during the downstroke start from the wing tip, around which the LEVs breaks down. Vortex tube (VT) wrapped inside the LEVs is found during the downstroke and are released between the downstrokes and the upstrokes to the wake. The WTVs made during the downstroke induce downward flow between the left and right WTVs and provide the lift to the butterfly. On the contrary, WTVs made during an upstroke induce streamwise flows and then provide the thrust. It can be found that the magnitudes of the forces below the VTs are large compared with those on the wings above which no vortical structures are seen. The pitching moment about the center of mass of the thorax is sensitive to the small structures on the wings such as the VTs. It indicates that the small structures can play a role in the free flight of the butterfly at the intermediate Reynolds number $O(10^3)$.

CONCLUSIONS

In this work, the flapping flights of the butterflies in the flow inflowing with the constant velocities are numerically simulated. The three kinds of the numerical simulations, the tethered simulation, the prescribed simulation and the free-flight simulation, are made. In the tethered simulation, the upward and streamwise forces of the simulation agree with those of the experiment. On the other hand, the tracers in the flow in the simulation shows zig-zag patterns similar to those in the experiment. In the prescribed simulation, the control to stabilize periodic flights is energy-efficient since the powers done by the extra forces to realize the observed trajectory are much smaller than the works due to the controllable joints. The characteristic vortical structures are found in the wakes. The wing-tip vortices made during the downstrokes provide the lift and those during the upstrokes provide the thrust. The pitching moment about the center of mass of the thorax depends strongly on the complex vortical structures on the wings behind the leading-edge vortices separated on the leading edges. The free-flight simulation in this work fails to make a stable periodic flight. The butterfly in the simulation cannot maintain the pitching angle of the thorax in a proper range and the pitching angle is the key to the stable periodic flights. The flapping flights of the butterfly appear to be unstable and the control of the pitching angle is essential.

References

[1] Vogel S., Alexander D.E.: Nature's flyers: birds, insects, and the biomechanics of flight. Johns Hopkins Univ. Pr., 2004.

[2] Brodsky A.K.: Vortex formation in the tethered flight of the peacock butterfly inachis io l. (lepidoptera, nymphalidae) and some aspects of insect flight evolution. *J. Exp. Biol.*, **161**:77–95, 1991.

[3] Dickinson M.H., Götz K.G.: The wake dynamics and flight forces of the fruit fly drosophila melanogaster. *J. Exp. Biol.*, **199**:2085–2104, 1996.

[4] Ellington C.P., Berg C.V.D., Willmott A.P., Thomas A.L.R.: Leading-edge vortices in insect flight. *Nature*, **384**:626–630, 1996.

[5] Wang X.X., Wu Z.N.: Stroke-averaged lift forces due to vortex rings and their mutual interactions for a flapping flight model. *J. Fluid Mech.*, **654**:453–472, 2010.

[6] Mittal R., Iaccarino G.: Immersed boundary methods. *Annu. Rev. Fluid Mech.*, 37:239–261, 2005.